Photosynthesis Research (2022) 154:291–302
https://doi.org/10.1007/s11120-022-00942-7

ORIGINAL ARTICLE

Dynamic Stark effect in *β* and *γ* carotenes induced by photoexcitation of bacteriochlorophyll *c* in chlorosomes from *Chloroflexus aurantiacus*

Andrei G. Yakovlev[1] · **Alexandra S. Taisova**[1] · **Zoya G. Fetisova**[1]

Received: 19 January 2022 / Accepted: 20 July 2022 / Published online: 17 September 2022

Abstract

Chlorosomes of green bacteria can be considered as a prototype of future artificial light-harvesting devices due to their unique property of self-assembly of a large number of bacteriochlorophyll (BChl) *c/d/e* molecules into compact aggregates. The presence of carotenoids (Cars) in chlorosomes is very important for photoprotection, light harvesting and structure stabilization. In this work, we studied for the first time the electrochromic band shift (Stark effect) in Cars of the phototrophic filamentous green bacterium *Chloroflexus* (*Cfx.*) *aurantiacus* induced by fs light excitation of the main pigment, BChl *c*. The high accuracy of the spectral measurements permitted us to extract a small wavy spectral feature, which, obviously, can be associated with the dynamic shift of the Car absorption band. A global analysis of spectroscopy data and theoretical modeling of absorption spectra showed that near 60% of Cars exhibited a red Stark shift of ~ 25 cm^{-1} and the remaining 40% exhibited a blue shift. We interpreted this finding as evidence of various orientations of Car in chlorosomes. We estimated the average value of the light-induced electric field strength in the place of Car molecules as ~ 10^6 V/cm and the average distance between Car and the neighboring BChl *c* as ~ 10 Å. We concluded that the dynamics of the Car electrochromic band shift mainly reflected the dynamics of exciton migration through the chlorosome toward the baseplate within ~ 1 ps. Our work has unambiguously shown that Cars are sensitive indicators of light-induced internal electric fields in chlorosomes.

Keywords Photosynthesis · Chlorosome · *Chloroflexus aurantiacus* · Carotenoid · Stark effect · Pump-probe spectroscopy

Abbreviations

BChl	Bacteriochlorophyll
Car	Carotenoid
Cfx	*Chloroflexus*
Chl	Chlorophyll
CMC	Chlorosome-membrane complex
DAS	Decay-associated spectrum
EET	Excitation energy transfer
ESA	Excited state absorption
GSB	Ground state bleaching
GVD	Group velocity dispersion
LHC	Light-harvesting complex
RC	Reaction center
SE	Stimulated emission

Introduction

Photosynthesis in green bacteria is initiated by the absorption of sunlight by chlorosomes, unique extramembrane organelles consisting mainly of self-aggregated bacteriochlorophylls (BChls) *c*, *d* or *e* (for reviews, see (Frigaard and Bryant 2006; Mirkovic et al. 2017; Oostergetel et al. 2010; Bryant and Canniffe 2018) and references therein). The excited state energy of BChls is finally transferred to the reaction centers for charge separation. Unlike other light-harvesting complexes (LHCs), chlorosomal BChls are aggregated by self-assembly (Krasnovsky and Bystrova 1980; Smith et al. 1983). This property makes chlorosomes very attractive for study as a prototype of future artificial LHCs. The protein-lipid sack envelops the BChl aggregates. Together with the baseplate, this sack maintains the ellipsoidal shape of chlorosomes. Carotenoids (Cars), quinones and small amounts of BChl *a* (in the baseplate) are also found in chlorosomes. The atomistic 3D structure of chlorosomes is unknown yet, but various structural elements such as rods (Staehelin et al. 1978), lamellas (Pšenčik et al. 2004) and helices (Ganapathy et al. 2009) were proposed as building

✉ Andrei G. Yakovlev
yakov@genebee.msu.ru

[1] Belozersky Institute of Physico-Chemical Biology, Lomonosov Moscow State University, Leninskie Gory, 119991 Moscow, Russian Federation

blocks for them. A complicated mixture of these elements in native chlorosomes has been proposed (Günther et al. 2016).

The presence of Cars in LHCs is very important for light harvesting, photoprotection, and structure stabilization (for reviews, see (Frigaard and Bryant 2006; Mirkovic et al. 2017; Polivka and Sundström 2004; Hashimoto et al. 2018) and references therein). Femtosecond time-resolved spectroscopy showed a high rate of excitation energy transfer (EET) from Cars to (B)Chls in LHCs which means the close proximity between them. As a consequence of their molecular structure and spectroscopic properties, free Cars in solutions and Cars in LHCs exhibit a large electrochromic shift (Stark effect) of absorption bands in an external electric field (Krawczyk and Olszówka 2001; Frese et al. 1997, 2002; Palacios et al. 2003). The direction of this shift to either blue or red depends on the mutual orientation of the electric field and the dipole moment of the Car molecule (Bublitz and Boxer 1997). For random orientations of fixed molecules, the first and second derivatives of the ground state spectrum of isolated absorption band contribute to the Stark spectrum. For example, a typical Stark spectrum of β carotene in a solvent can be well fitted by the first derivative with a small addition of the second derivative, both of which are approximately periodical functions of the wavenumber (Krawczyk and Olszówka 2001). A much more complicated Stark lineshape is observed in the Soret/Car absorption band of *Cfx. aurantiacus* chlorosomes (Frese et al. 1997). In this case, a detailed comparison of the Car-containing and Car-less samples is necessary to adequately explain the observed Stark spectrum. An analysis of the Stark spectra made it possible to estimate the differences in the polarizability, $\Delta\alpha$, and the permanent dipole moment, $\Delta\mu$, between the ground and excited states. For example, $\Delta\alpha = 1000–1300$ Å$^3/f^2$ and $\Delta\mu = 5–6$ D/f for β carotene in different solvents (D–Debye, f = internal electric field/external electric field) (Krawczyk and Olszówka 2001). Estimations of the same order were obtained for Cars of *Cfx. aurantiacus* chlorosomes: $\Delta\alpha = 1600–1900$ Å$^3/f^2$ and $\Delta\mu = 4–7$ D/f (Frese et al. 1997).

It was found that the fs light excitation of BChls causes the ultrafast shift of the Car absorption band in the LHCs (Herek et al. 1998, 2004; Gottfried et al. 1991a; Pinnola et al. 2016). This effect was observed in LH2 complexes of *Rhodobacter sphaeroides* containing neurosporene (Herek et al. 1998) and in *Rhodopseudomonas acidophila* containing rhodopin glucoside, in *Rhodospirillum molischianum* containing lycopene and *Rhodobacter sphaeroides* containing lycopene (Herek et al. 2004). In these experiments, the Q_y bands of B800 or B850 were excited, and the Cars S_2 absorption bands were probed. The Car band shift appeared instantaneously with the pump pulse and then decayed on the ps time scale. A correlation between the dynamics of the Car band shift and the dynamics of B800 → B850 EET was found. For example, the major decay component of the Car kinetics (~ 1.3 ps) was close to the B800 decay time (~ 1.2 ps) for *Rhodobacter sphaeroides* LH2 at 77 K (Herek et al. 1998). The authors concluded that the Car band shift is the result of a change in the local electric field. This idea was first advanced in the sub-ps spectroscopy study of LHCs (Gottfried et al. 1991a). Quantum chemical calculations have shown that the mutual spatial orientation of pigments in LH2 determines the magnitude of the Car band shift. The strength of the static local electric field in the vicinity of Car was estimated as 4–6 MV/cm. In the ppLHCSR1 complexes from the moss *Physcomitrella patens*, wavelike ΔA spectra were observed in the spectral region of the violaxanthin and zeaxanthin absorption bands upon excitation of the Q_y absorption band of Chl *a* (Pinnola et al. 2016). The major times of the multi-exponential decays of this wavy pattern and Chl *a* Q_y band were 1.5 and ~ 4 ps, respectively, at pH = 7. The authors explained the changes in the Cars bands by their light-induced electrochromic shift. Conversely, excitation of Chl *a* did not cause a Stark shift of the lutein band in trimeric LHCII from spinach (Gradinaru et al. 2003). The authors observed a slight bleaching of lutein molecules upon Chl *a* excitation and ascribed this to excitonic mixing of the lutein and Chl *a* electronic states. Probably, a complicated mixture of the Soret absorption bands of Chl *a* and Chl *b* and absorption bands of lutein and neoxanthin masked the weak band shifts of these two Cars in LHCII from spinach.

A dynamic shift of the Car absorption band was also observed in photosynthetic reaction centers (RCs) (Romero et al. 2011; Paschenko et al. 2012; Gottfried et al. 1991b). In RCs, electrochromic absorption changes are caused by both excitation of (B)Chls and charge separation (Gottfried et al. 1991b). In the photosystem II RCs of higher plants, a wavy pattern of transient ΔA spectra was observed in the spectral region of β carotene absorption within ~ 20 ps after excitation of peripheral chlorophylls $Chls_Z$ (Romero et al. 2011). The negative ΔA features at ~ 465 and ~ 490 nm and positive features at ~ 485 and ~ 500 nm were explained by 5-nm blue electrochromic shift of the Car band. The correlation between excitation of $Chls_Z$ and the shift of the Car S_2 band may result from the close proximity of Car and $Chls_Z$ or even shows a mixing of their electronic states. In isolated RCs from the purple bacterium *Rhodobacter sphaeroides*, an extremely fast (~ 30 fs) dynamics was observed in the S_2 absorption band of the spheroidene upon excitation at 600 nm where monomeric and dimeric BChls have Q_x bands (Paschenko et al. 2012). A wavelike form of the transient ΔA spectrum well repeated the second derivative of the Car absorption band. The authors ascribed this effect to an electrochromic band shift of the Car in the local electric field of the excited B_B molecule. The rapid $Q_x \rightarrow Q_y$ internal conversion in the B_B leads to a change of the dipole moment acting

on the neighboring Car. As a result, about half of the Car molecules exhibit a red shift of their absorption bands while the other half exhibits a blue shift of the same magnitude.

Herein, we studied the early-time dynamics of the Car absorption band of chlorosomes from the phototrophic filamentous anoxygenic green bacterium *Cfx. aurantiacus* caused by 20-fs light excitation of the Q_y band of BChl *c* at room temperature. We observed a small wavy spectral feature in the region of Car absorption, which is superimposed on the Soret band bleaching. The magnitude of this feature depended on the Car content. Analysis of the spectroscopy data showed that the wavy feature decayed within ~ 1 ps. We ascribed the observed phenomenon to the electrochromic shift (Stark effect) of the Car absorption band due to the internal electric field of the excited BChl *c*. We explained the dynamics of this shift by the migration of excitation energy in chlorosomes. To our knowledge, this is the first report on the light-induced Stark effect in chlorosomes.

Materials and methods

Samples

The object of the study was the green bacterium *Cfx. aurantiacus* strain Ok-70-fl (collection of Leiden University, The Netherlands). *Cfx. aurantiacus* cells were cultured anaerobically at 55 °C in batch cultures at a light intensity of ~ 3 μE/(m^2 s) (low-light intensity) and ~ 60 μE/(m^2 s) (high-light intensity). Chlorosome-membrane complexes (CMC) were obtained from freshly grown cell cultures according to the method of (Ma et al. 1996) in some modification. Bacterial cells were centrifuged at 8,500 × g for 20 min, washed twice with 10 mM Tris–HCl buffer, pH 8.0, and suspended in TA buffer (10 mM Tris–HCl buffer, 10 mM sodium ascorbate, pH 8.0). The suspension was broken by passing twice through a French press cell at 20,000 psi in the presence of 2 mM phenylmethylsulfonyl fluoride. Intact cells and large pieces of cells were removed by centrifugation at 20,000 × g for 30 min at 4 °C. CMC were isolated from the obtained supernatant by centrifugation for 90 min at 180,000 × g (45,000 rpm, Ti 50) at 4 °C, and the resulting pellet was resuspended in a small volume of the TA buffer. Chlorosomes were isolated from fresh (not frozen) suspension of *Cfx. aurantiacus* CMC in TA buffer in a two-fold sequential continuous sucrose gradient (first 55–20% (w/w), then 45–15% (w/w), as previously described in the modification of chlorosome isolation from CMC (Taisova et al. 2002). For this, continuous density gradients were prepared in 50 mM Tris–HCl buffer, pH 8.0, with 2 M NaSCN (tris-thiocyanate buffer) in the presence of 10 mM sodium ascorbate in 38 ml centrifuge tubes. CMC suspension (1.5–2.0 ml, OD = 150–170 at 740 nm) was applied over each sucrose gradient. The tubes were centrifuged for 20 h at 135,000 × g (28,000 rpm, SW-28) at 4 °C and then chlorosomes absorbing at 740 nm were collected between sucrose gradients from 28 to 30%. It should be noted that only freshly isolated chlorosomes were used in the experiments. Before measurements, chlorosomes were incubated for 30 min with 18 mM sodium dithionite at 4 °C to ensure highly reduced conditions.

Spectroscopy

Details of spectroscopy measurements are available in (Yakovlev et al. 2020, 2021). Shortly, 20-fs light pulses (Ti:sapphire laser, Spectra Physics, USA) were stretched up to ps duration, amplified (multi-pass Ti:sapphire amplifier, Avesta, Russia), and compressed back to fs duration. A smooth white-light continuum was obtained by focusing the amplified pulses into ethylene glycol (thin flat jet). After spatial filtering, the continuum was divided into a small part (probe light) and a main part (pump light, λ ~ 740 nm). The pump-probe delay was set with an accuracy of 1 fs and varied from − 0.1 to 20 ps with a step of 25-fs. A combination of a monochromator and an optical multichannel analyzer (Oriel, France) was used to collect and record the probe light that passed through the sample. Group velocity dispersion (GVD) was minimized by a 4-prism compensator. We measured the bleaching of colored glasses (LOMO, St.-Petersburg, Russia) to estimate the residual GVD (≤ 30 fs) and correct the experimental time scale. The pump-probe cross-correlation had a duration of 25 fs. To avoid nonlinear effects, the pump intensity was properly attenuated to excite less than ~ 20% of chlorosomes. The typical value of the excitation intensity was ~ 2×10^{12} photons per cm^2 per pulse which corresponds to the case of weak annihilation (Yakovlev et al. 2021). The pump and probe beams were polarized at a magic angle (54.7°) with respect to each other. Several thousands of time-resolved Δ*A* (light − dark) spectra were collected at a 40-Hz repetition frequency and averaged at each pump-probe delay. The improved stability of the laser system resulted in a high accuracy of Δ*A* measurements ($\leq 10^{-5}$). Global analysis was applied to the $\Delta A(\lambda, t)$ manifold to extract kinetic time constants and decay-associated spectra (DAS). The samples had OD = 0.5 at λ = 740 nm in a 1-mm cuvette. To avoid heating of the sample, the cuvette was moved forward and back in its plane. A Hitachi-557 spectrometer (Japan) was used to measure the ground state absorbance. Spectroscopy measurements were performed at 293 K.

Results and discussion

Spectroscopy data

Figure 1 shows the blue-green regions of the ground state absorption spectra of two samples of *Cfx. aurantiacus* chlorosomes prepared from cells cultivated at low (~ 3 μE/

(m^2 s)) and high (~60 μE/(m^2 s)) intensities of light. The spectra were normalized at 570 nm. We avoided the normalization to the Q_y or the Soret bands due to their different hyperchromism (in the Q_y) or hypochromism (in the Soret) in chlorosomes grown at different light intensities (Yakovlev et al. 2020). The spectral region at 570 nm is far from both absorption bands and thus appears to be more favorable for normalization. Both spectra in Fig. 1 consist of a strongly overlapping Soret band of aggregated BChl *c* and an absorption band of Car (mostly *β* and *γ* carotenes). The spectra have a peak at ~457 nm and two broad shoulders at ~420 and ~500 nm. The difference of the two spectra (Fig. 1B) resembles the well-known absorption spectrum of *β* carotene in solvent (Krawczyk and Olszówka 2001). In line with the previous report (Yakovlev et al. 2002), this means that the Car content in chlorosomes increases when more intense light is used to grow bacteria. This statement is confirmed by pigment analysis of *Cfx. aurantiacus* chlorosomes cultivated at different illuminations (Ma et al. 1996), and by comparison of the absorption spectra of the so-called low-light and high-light chlorosomes containing the same amount of BChl *c* (Yakovlev et al. 2021). The peaks at ~497, ~467 and ~443 nm in the difference spectrum most probably represent the 0–0, 0–1 and 0–2 bands of the active high-frequency mode of Car, respectively (Polivka and Sundström 2004). The ground state spectrum of Car-deficient *Cfx. aurantiacus* chlorosomes treated by hexane had no shoulder at ~500 nm while the central peak and the shoulder at ~420 nm exhibited minor changes (Melø et al. 2000). The full absorption spectrum of *Cfx. aurantiacus* chlorosomes contains, in addition to the Soret/Car band, a strong Q_y band of BChl *c* at ~740 nm and a small BChl *a* band at ~795 nm (Fig. S1).

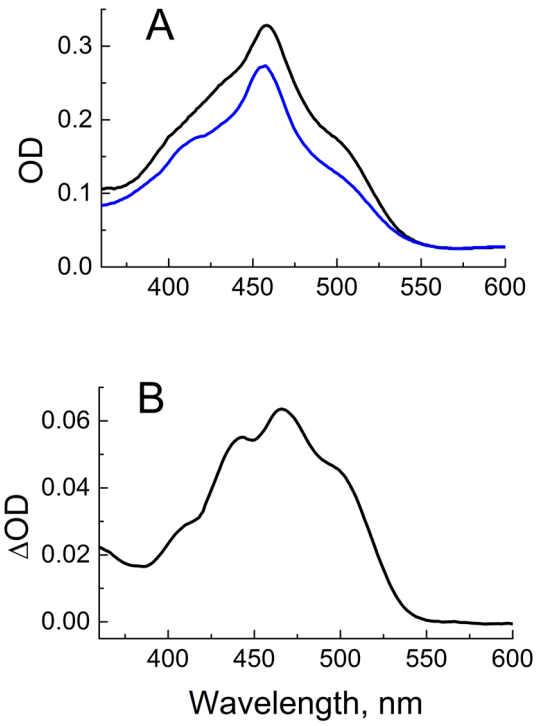

Fig. 1 Steady-state Soret/Car absorption bands (**A**) and their difference (**B**) of *Cfx. aurantiacus* chlorosomes prepared from cells cultivated at ~3 μE/(m^2 s) (blue) and ~60 μE/(m^2 s) (black) intensities of light. The spectra are normalized at 570 nm

We varied pump-probe delay from − 0.1 to 20 ps with a 25-fs step and measured the Δ*A* (light – dark) spectra at each delay. Figure 2 shows some representative Δ*A* spectra of chlorosomes prepared from cells cultivated at high and low intensities of light and excited at ~740 nm (maximum of the BChl *c* Q_y absorption band). In the region of the Soret/Car absorption band, a negative Δ*A* signal appeared simultaneously with the pump pulse due to the BChl *c* ground state bleaching (GSB), and then it partially decayed on a ~10-ps time scale.

Due to the increased stability of the laser system, the signal-to-noise ratio of spectral measurements was high enough to reliably record $\Delta A \leq 10^{-5}$. This allowed us to find small additional features such as a negative shoulder at ~495 nm and a positive peak at ~530 nm on the red side of the negative Δ*A* signal (see Δ*A* spectrum at 50-fs delay). These features appeared at the same time with the pump pulse (see Δ*A* spectrum at zero delay) and completely disappeared after a few ps (see Δ*A* spectrum at 10-ps delay). This wavelike spectral pattern is considerably weaker in the Δ*A* spectra of chlorosomes containing less Car (prepared from cultures grown at low intensity of light, Fig. 2B) than in the Δ*A* spectra of

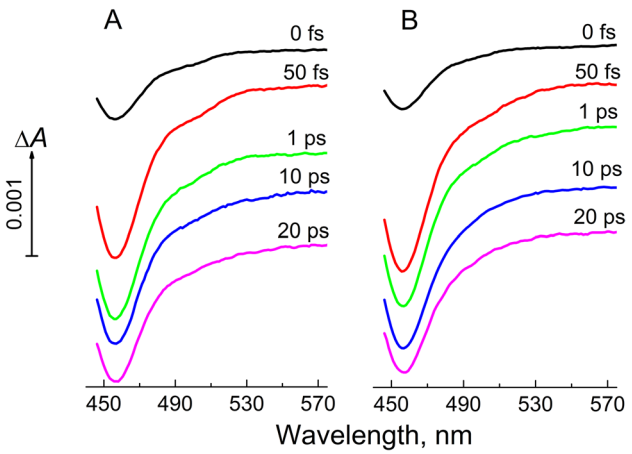

Fig. 2 Blue-green spectral regions of typical transient Δ*A* (light − dark) spectra of *Cfx. aurantiacus* chlorosomes prepared from cells cultivated at ~60 μE/(m^2 s) (**A**) and ~3 μE/(m^2 s) (**B**) intensities of light. Delay times (in ps and fs) between the pump and probe pulses are shown in numbers. The spectrum of pump pulses was at ~740 nm (the maximum of the Q_y absorption band). The spectra are vertically shifted for clarity. For each spectrum, $\Delta A \rightarrow 0$ at λ ~570 nm

chlorosomes containing more Car (prepared from cultures grown at high intensity of light, Fig. 2A). This means that the wavy features originate from the Car absorption band. At first sight, the wavy features look like the bleaching of the S_2 absorption band of Car at ~ 495 nm (0–0 vibrational transition) and the excited state absorption (ESA) from the Car S_1 state at ~ 530 nm (Polivka and Sundström 2004; Hashimoto et al. 2018; Yakovlev et al. 2021). However, the following considerations do not prove this statement. First, the pump wavelength of 740 nm used in the present work excluded the direct excitation of Car. The simultaneous bleaching of the Car and BChl *c* absorption bands could be due to the exciton interaction between these pigments, but this is not the case for *Cfx. aurantiacus* chlorosomes, although the extremely fast Car → BChl *c* EET shows a close proximity between Car and aggregated BChl *c* (Yakovlev et al. 2021). Second, in *Cfx. aurantiacus* chlorosomes, direct Car excitation at ~ 500 nm leads to a negative ΔA signal of GSB and stimulated emission (SE) at ~ 510 nm and a positive ΔA signal of ESA at ~ 550 nm (Yakovlev et al. 2021). In this case, the ESA signal is delayed by ~ 70 fs with respect to the GSB/SE signal due to the population of the Car S_1 state from the initially excited S_2 state. The Car S_1 state has a lifetime of ~ 10 ps in *Cfx. aurantiacus* chlorosomes. In contrast, the features observed at ~ 495 and ~ 530 nm in the present work exhibit simultaneous appearance and a lifetime considerably shorter than 10 ps. Based on the literature (see Introduction), we assumed the presence of an electrochromic shift of the Car absorption band induced by excitation of BChl *c*.

For more details, a global analysis was applied to the whole set of $\Delta A(\lambda, t)$ spectra. We focused on early-time events that occurred within several ps after excitation and limited the time window of the analysis by 20 ps. After deconvolution with a 25-fs instrumental response function, ΔA kinetics were approximated at each λ by exponential functions. The resulting decay-associated ΔA spectra (DAS) are shown in Fig. 3. At least four exponentials with time constants of 0.1–0.2, 0.4–0.6, 0.9–1.4 and 9–12 ps were needed for a good approximation of the ΔA kinetics in the entire spectral region of measurements. The ranges of the time constants reflect the overall accuracy ~ 7% of the fitting. Simultaneous variation of the time constants within these ranges did not change the residual (i.e., the difference between the kinetics and the fit) at each λ by more than 7%. This set of exponentials was not unique: a satisfactory fit could be obtained with five exponentials, and a worse fit could be performed with three exponentials. We did not find components longer than 12 ps due to the limited time window (20 ps) of measurements. GSB of BChl *c* decayed slightly within this time window and, consequently, longer kinetic components (represented by a constant background in our analysis) dominated in the Soret band. The weak 0.4–0.6 ps component can be associated with the blue shift

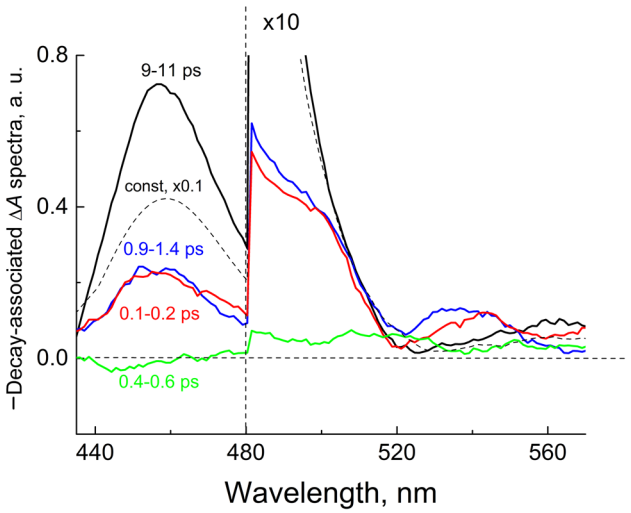

Fig. 3 Decay-associated ΔA spectra obtained from a global analysis of the $\Delta A(\lambda, t)$ spectra in the blue-green spectral region with a time window of 20 ps. The spectra were multiplied by 10 and additionally smoothed for $\lambda > 480$ nm. Dashed line: component with infinitely long decay, multiplied by 0.1

of the Soret band, for example, due to vibrational relaxation in the ground state of BChl *c* or energy redistribution between the Soret sub-bands. The other three decay components represent the partial recovery of the BChl *c* ground state and the decay of wavelike spectral features. Among them, the 9–11 ps decay component dominated at $\lambda < 500$ nm, but at longer wavelengths all three decay components had similar amplitudes. It should be noticed that the decay components reported here are approximately similar to those obtained in the analysis of the Q_y absorption band dynamics in *Cfx. aurantiacus* chlorosomes (Savikhin et al. 1994; Yakovlev et al. 2021). Excitation of BChl *c* either to the Q_y or Soret band initiates an exciton migration between different structural elements of the aggregated BChl *c* with subsequent EET to the baseplate BChl *a* (Prokhorenko et al. 2000; Linnanto and Korppi-Tommola 2008, 2012). In addition, the fastest (~ 0.1 ps) component can contains coherent signals of different origin. Thus, in our study, the dynamics of GSB reflected the loss of excitation in BChl *c*.

To reveal the pure dynamics of the wavelike spectral features, we subtracted the normalized ΔA spectrum recorded at 20 ps from all $\Delta A(\lambda, t < 20$ ps) spectra. This subtraction mainly removes the pure spectrum of BChl *c* GSB from the ΔA spectra. Several typical $\Delta\Delta A$ spectra are shown in Fig. 4. The picture of the normalized spectra before subtraction is presented in the Supplement as Fig. S2. A similar wavy shape is clearly seen in the spectra recorded at 0, 0.05 and 1 ps. The amplitudes of the positive band at ~ 530 nm and negative bands at ~ 496 and ~ 450 nm are ~ 2.5 times greater in the spectra of chlorosomes with a higher Car content, isolated from cells grown at high

intensity of light. It can be seen from Fig. 4 that the whole $\Delta\Delta A$ signal decayed within a few ps. For comparison, the Stark spectrum of *Cfx. aurantiacus* chlorosomes has positive peaks at ~ 533, ~ 493, ~ 470 and ~ 420 nm and negative peaks at ~ 585, ~ 513, ~ 478 and ~ 455 nm (Frese et al. 1997). The Stark spectrum of all-trans β,β carotene in a solvent has positive peaks at ~ 517, ~ 481 and ~ 450 nm and negative peaks at ~ 500, ~ 465 and ~ 435 nm (Krawczyk and Olszówka 2001). The shape of our $\Delta\Delta A$ spectra more resembles the Stark spectrum of pure Car than the Stark spectrum of *Cfx. aurantiacus* chlorosomes. Probably, the external electric field caused the Stark shift of both the BChl and Car bands in the spectra of chlorosomes. It should be noted that usually Stark spectroscopy is performed on frozen samples at cryogenic temperature.

Next, the procedure of global analysis was applied to the $\Delta\Delta A(\lambda, t)$ manifold. The corresponding DAS are shown in Fig. 5. Four exponential components contributing to the decay of the $\Delta\Delta A$ signal are the same as those found by global analysis of the $\Delta A(\lambda, t)$ spectra (see Fig. 3). No additional exponentials were required for a good approximation of the $\Delta\Delta A(\lambda, t)$ spectra. This is an argument in favor of the existence of the same process causing the BChl *c* and Car dynamics mainly represented in the ΔA and $\Delta\Delta A$ spectra, respectively. Presumably, this is the EET between the BChl *c* oligomers and from them to the baseplate BChl *a*. In contrast to ΔA DAS, $\Delta\Delta A$ DAS showed the major contribution of two fast components with time constants of 0.1–0.2 and 0.9–1.4 ps. The spectra of these components have two extrema at ~ 495 and ~ 535 nm, roughly corresponding to two extrema in the $\Delta\Delta A$ spectra. The weak 0.4–0.6 ps component probably represents the blue shift of the $\Delta\Delta A$ signal.

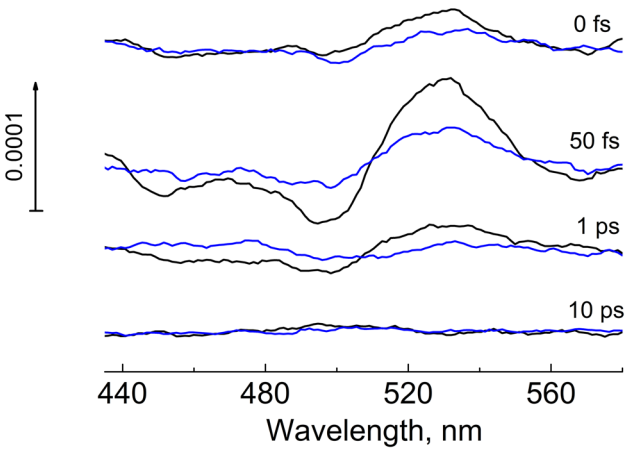

Fig. 4 Typical double difference spectra obtained by subtraction the normalized ΔA spectrum measured at 20 ps from the $\Delta A(\lambda, t)$ spectra. Delay times (in ps and fs) between the pump and probe pulses are shown in numbers. Black(blue): samples of chlorosomes prepared from cells cultivated at ~ 60(3) μE/(m^2 s). The spectra are vertically shifted for clarity

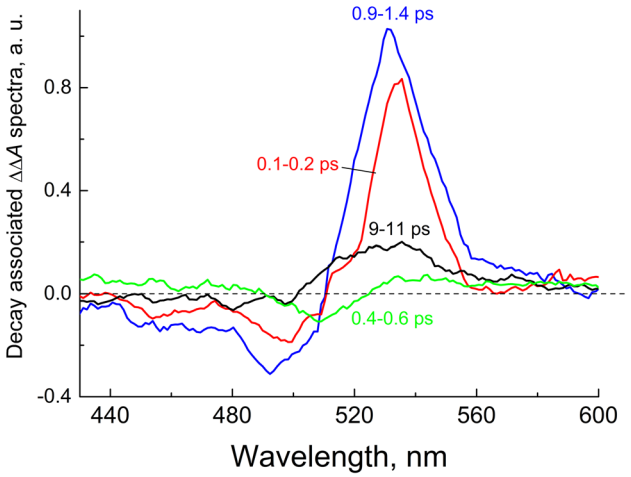

Fig. 5 Decay-associated $\Delta\Delta A$ spectra obtained from a global analysis of the transient $\Delta\Delta A$ spectra of chlorosomes from *Cfx. aurantiacus*. See text for details

To illustrate the decay of the $\Delta\Delta A$ signal, we plotted the corresponding kinetics at four wavelengths (Fig. 6). Positive kinetics at 525 and 540 nm and negative kinetics at 480 and 500 nm showed the main decay with a similar time ~ 1 ps.

Estimation of light-induced Stark effect

Next, we tried to simulate the observed $\Delta\Delta A$ spectra, assuming that they mainly represent the absorption spectra of Cars. It is known that two types of Car, β and γ carotenes, are mostly present in approximately equal amounts in *Cfx. aurantiacus* chlorosomes (Halfen et al. 1972; Takaichi 1999). The absorption spectrum of γ carotene is similar to the absorption spectrum of β carotene, but is shifted

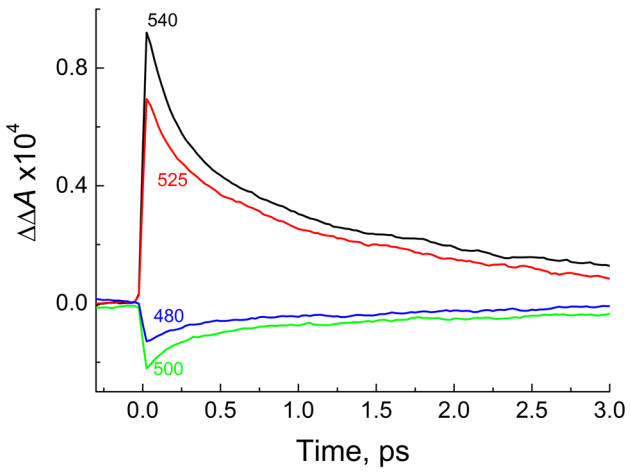

Fig. 6 Typical $\Delta\Delta A$ kinetics of chlorosomes from *Cfx. aurantiacus* cells at 480, 500, 525 and 540 nm. See text for details

to the red by ~ 10 nm (Fuciman et al. 2010). We fitted the ground state absorption spectra of both carotenes by the sum of three Gaussians as follows:

$$A_{\beta,\gamma} = \sum_{i=1}^{3} A_{\beta,\gamma^i} \cdot \exp\left(-\frac{(\upsilon - \upsilon^{0,i_{\beta,\gamma}})^2}{\delta\upsilon^{i_{\beta,\gamma^2}}}\right) \quad (1)$$

The Stark-shifted spectra can be written as

$$A_{\beta,\gamma^{\pm Stark}} = \sum_{i=1}^{3} A_{\beta,\gamma^i} \cdot \exp\left(-\frac{(\upsilon - \upsilon^{0,i_{\beta,\gamma}} \pm \delta\upsilon_{\beta,\gamma^{i,Stark}})^2}{\delta\upsilon^{i_{\beta,\gamma^2}}}\right) \quad (2)$$

where $\pm\delta\upsilon_{\beta,\gamma}^{\ i,Stark}$ corresponds to red (+) and blue (−) shifts. If we assume that a part ($P_{\beta,\gamma}$) of Car molecules has an absorption spectrum shifted to the red side, and the other part ($1 - P_{\beta,\gamma}$) has a blue-shifted spectrum, then the experimental $\Delta\Delta A$ signal is proportional to the following difference:

$$\Delta\Delta A \sim \sum_{\beta,\gamma} \left(P_{\beta,\gamma}\left(A_{\beta,\gamma}^{+Stark} - A_{\beta,\gamma}\right) + \left(1 - P_{\beta,\gamma}\right)\left(A_{\beta,\gamma}^{-Stark} - A_{\beta,\gamma}\right)\right) \quad (3)$$

Parameters used for the best fit are listed in Table 1, and the calculated ground state and differential spectra are shown in Fig. 7.

The sum of A_β and $A\gamma$ described well the experimental Car absorption spectra taken from Fig. 1B at $\lambda > 440$ nm (Fig. 7A). To calculate the Stark-shifted absorption spectra of both Cars, we changed the absorption maximum of the red-most Gaussian by ± 35 cm^{-1}, and the maxima of other Gaussians by ± 15 cm^{-1}. We assumed that 57% of β-Car and 62% of γ-Car molecules exhibit a red electrochromic shift, while the remaining 43% of β-Car and 38% of γ-Car have a shift of the same magnitude to the blue side. The sum of the calculated differences between the Stark-shifted and original absorption spectra of β and γ Cars is in satisfactory agreement with the experimental $\Delta\Delta A$ spectrum at $\lambda > 460$ nm (Fig. 7B) and a delay time of 50 fs. At later times, the same fitting is applicable with smaller spectral shifts consistent with the $\Delta\Delta A$ kinetics (see Figs. 4 and 6). This fitting is not unique: the simultaneous change of P and $\delta\upsilon^{\ Stark}$ by 4–6% and A, υ and $\delta\upsilon$ by ~ 2% did not change the overall closeness between the experimental and calculated curves in Fig. 7.

Thus, the shape of the small wavy features observed in the ΔA spectra of chlorosomes from *Cfx. aurantiacus* at 460 nm < λ < 550 nm can be explained by the shift of the β-Car and γ-Car absorption bands due to impulse light excitation of BChl *c*. Comparable contributions of red-shifted and blue-shifted Car molecules indicate a broad variety of their orientations with respect to the light-induced electric field. It should be noted that the shifts of 15 cm^{-1} (~ 0. 4 nm at $\lambda = 500$ nm) and 35 cm^{-1} (~ 0.9 nm at $\lambda = 500$ nm) obtained in the present work are several times smaller than a blue shift of 3–4 nm reported for the light-induced Stark effect in LH2 complexes of purple bacteria (Herek et al. 2004) and a 5-nm blue light-induced Stark shift in the photosystem II RCs of higher plants (Romero et al. 2011). The authors explained the large blue Stark shift by the presence of a strong static local field generated by proteins with a direction opposite to the light-induced electric field. The absence of a large amount of proteins in chlorosomes can lead to a smaller light-induced Stark shift in them.

It is unclear why the red part ($\lambda \geq 490$ nm) of the Car absorption band exhibits a larger Stark shift than the central part ($\lambda \leq 490$ nm) in our work. It seems unlikely that the 0–0 transition of high-frequency active modes is more sensitive to the electric field than the 0–1 and 0–2 transitions. Probably, this observation shows that β-Car and γ-Car contribute unequally to the Stark shift in spite of their close contribution to the absorption spectrum. Different values of the Stark shift (± 15 and ± 35 cm^{-1}) can be alternatively explained by the structural heterogeneity of chlorosomes. Probably, Cars are located in at least two different structures of BChl aggregates such as, for example, rods and lamellae. The electric fields generated by light excitation of these structures would undoubtedly be different. It seems impossible to check these possibilities carefully without exact knowledge of the spatial

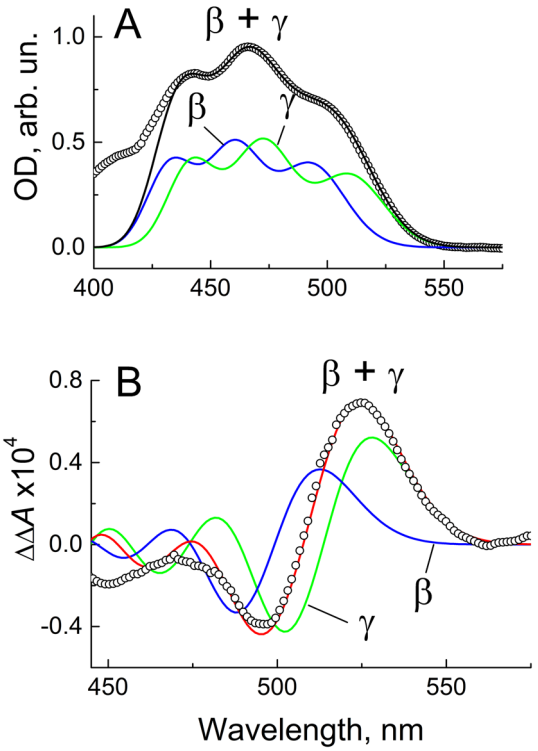

Fig. 7 Fitting of the ground state **(A)** and ΔΔA **(B)** spectra of Cars from *Cfx. aurantiacus* chlorosomes by the sum of β-Car and γ-Car spectra. Circles are experimental data, solid curves are simulation. In panel **B**, the delay time of the experimental data is 50 fs. See text for details

Table 1 Parameters used for the best fit of the Car ground state and Stark-shifted spectra. See Fig. 7 and text for details

i	A_β^i	$\upsilon^{0,i}{}_\beta$, cm^{-1}	$\delta\upsilon^i{}_\beta$, cm^{-1}	$\delta\upsilon_\beta{}^{i,Stark}$, cm^{-1}	P_β	A_γ^i	$\upsilon^{0,i}{}_\gamma$, cm^{-1}	$\delta\upsilon^i{}_\gamma$, cm^{-1}	$\delta\upsilon_\gamma{}^{i,Stark}$, cm^{-1}	P_γ
1	0.387	20,260	790	±35	57%	0.338	19,610	760	±35	62%
2	0.48	21,700	770	±15	57%	0.5	21,150	800	±15	62%
3	0.404	23,080	780	±15	57%	0.408	22,620	760	±15	62%

positions and orientations of Cars with respect to BChl aggregates. On the other hand, chlorosomes grown at high light and low light differ in many aspects, not only in the Car content. For example, they have different sizes of unit building blocks (Yakovlev et al. 2002). In this context, the extraction of the Car absorption band by simple subtraction of the low-light spectrum of chlorosomes from the high-light spectrum (Fig. 1B) seems not irreproachable. In addition, the subtraction of the normalized ΔA spectrum recorded at 20-ps pump-probe delay from each $\Delta A(\lambda, t < 20$ ps) spectrum is not free from possible artifacts due to a change of the form of the BChl *c* GSB spectrum with time. To check this possibility, we used the ΔA spectra recorded at 5, 10 and 15 ps for subtraction, and repeated the global analyses of the obtained $\Delta\Delta A$ spectra. The results of these procedures were the same as shown in Figs. 4–6. Thus, we believe that the larger Stark shift of the red part of the Car band is not an artifact and needs further study.

Discussion of Stark effect in chlorosomal Cars

An adequate theory of ultrafast light-induced electrochromic band shifts in the LHCs has not yet been created. A problem is much more complicated for the chlorosomes of green bacteria in which the exact atomistic structure is unknown. Therefore, the application of the theory of Stark spectroscopy is a possible way to qualitatively explain the results obtained. In Stark spectroscopy, a constant homogeneous electric field is usually applied to a sample in which isolated chromophores are surrounded by a polymer, protein or glass matrix. In chlorosomes excited by light, on the contrary, the light-induced internal electric field is essentially heterogeneous. Also, a protein matrix is absent in chlorosomes, and Car molecules are mainly surrounded by aggregated BChl *c*. Therefore, a direct application of the theoretical background used in Stark spectroscopy studies is not obvious in our case, and we will discuss this item below. Anyway, we tried to use the basic equation of Stark spectroscopy as it was done for the ultrafast Car band shift in LHCs (Herek et al. 2004) and RCs (Paschenko et al. 2012) of purple bacteria.

The electrochromic shift of the electronic transition frequency $\Delta\upsilon$ of an individual molecule in a homogeneous electric field $\boldsymbol{E}$ can be written as (Liptay 1974; Meixner et al. 1986; Rätsep et al. 1998):

$$\Delta\upsilon = -h^{-1}\left(\Delta\mu E + \Delta\alpha E_{loc}E + 0.5\Delta\alpha EE\right) \quad (4)$$

where $\Delta\boldsymbol{\mu}$ and $\Delta\alpha$ are the change in the dipole moment and polarizability, respectively, during an electronic transition; $\boldsymbol{E}_{\mathrm{loc}}$ – static local electric field; $\Delta\boldsymbol{\mu}$, $\boldsymbol{E}$ and $\boldsymbol{E}_{\mathrm{loc}}$ are vectors; $\Delta\alpha$ is a tensor; h is Planck constant. It is assumed in formula (4) that the total change in the dipole moment, $\Delta\boldsymbol{\mu}_{\mathrm{tot}}$, is a sum of the change in the molecular dipole moment, $\Delta\boldsymbol{\mu}$, and the change in the dipole moment caused by static local electric field, $\Delta\alpha\boldsymbol{E}_{\mathrm{loc}}$ (Rätsep et al. 1998). In our case, the electronic transition is the Car $S_0 \rightarrow S_2$ transition, $\boldsymbol{E}$ is the time-dependent change of the electric field at the position of the Car molecule due to the excitation of neighboring BChls. To obtain the macroscopic value of $\Delta\upsilon$, it is necessary to sum expression (4) overall Car molecules in each chlorosome and overall chlorosomes in the sample. Unfortunately, it is impossible without exact knowledge of the chlorosomal spatial structure, including the position and orientation of each Car molecule and the configuration of BChl aggregates. In the case of a random orientation of fixed molecules in a constant external electric field, the common expression (4) is converted into the well-known formula of Stark spectroscopy (Liptay 1974). This formula (also available in many works on Stark spectroscopy) shows that $\Delta\upsilon$ and the related ΔA are proportional to the sum of the first (scales with $\mathrm{Tr}(\Delta\alpha)$) and second (scales with $|\Delta\boldsymbol{\mu}|^2$) derivatives of the absorption spectrum. However, in our case, the orientation and position of Car are likely not random, and the microscopic electric field is not constant and homogeneous, but undoubtedly depends on the spatial structure of BChl *c* oligomers and the exciton dynamics. In this context, we can use formula (4) only for non-rigorous order-of-magnitude estimations.

Below we estimated the possible relative contributions of the terms from formula (4) separately. The first term in expression (4) produces either a red or a blue spectral shift depending on the mutual orientation of the $\Delta\boldsymbol{\mu}$ and $\boldsymbol{E}$ vectors. Taking $|\Delta\boldsymbol{\mu}| = 4$–$7$ *D* for Car from the Stark spectroscopy study of *Cfx. aurantiacus* chlorosomes (Frese et al. 1997) and assuming parallel or antiparallel orientation of $\Delta\boldsymbol{\mu}$ and $\boldsymbol{E}$, we neglected other terms and obtained $|\boldsymbol{E}| \sim 5 \bullet 10^5$ V/cm for the average experimental value $\Delta\upsilon \sim \pm 25$ cm^{-1}. The first term vanishes in the hypothetical case of random orientation of Car. The last term in (4) is responsible for the red shift of υ. Taking $\Delta\alpha = 1000$–2000 Å (Frese et al. 1997) and

$\Delta\upsilon \sim -25\ cm^{-1}$, we obtained $|\boldsymbol{E}| \sim 5 \bullet 10^6$ V/cm, if we neglect the first and second terms in (4). The second term can shift the Car absorption band either to the red or to the blue side depending on the mutual orientation of the $\boldsymbol{E}_{loc}$ and $\boldsymbol{E}$ vectors. It is likely that $\boldsymbol{E}_{loc}$ is not large in chlorosomes because of the absence of proteins. A small amount of proteins is located only in the protein-lipid envelope, and the majority of Car molecules are distant from them (Frigaard and Bryant 2006; Mirkovic et al. 2017; Oostergetel et al. 2010; Bryant and Canniffe 2018). The electric field $|\boldsymbol{E}_{loc}| \sim 5 \bullet 10^6$ V/cm was measured in proteins using the response of Car to the transmembrane potential (De Grooth and Amesz 1977). If we assume $|\boldsymbol{E}_{loc}| \sim |\boldsymbol{E}| \sim 3 \bullet 10^6$ V/cm in *Cfx. aurantiacus* chlorosomes and a near- parallel or antiparallel orientation of $\boldsymbol{E}_{loc}$ and $\boldsymbol{E}$, then we have an additional red or blue shift of υ by ~ 25 cm^{-1}. Thus, an order-of-magnitude estimation provides the value $|\boldsymbol{E}| \sim 10^6$ V/cm. It should be noticed that in the case of antiparallel orientation of $\boldsymbol{E}_{loc}$ and $\boldsymbol{E}$ the second and third terms in Eq. (4) compensates each other. The estimation obtained here for *Cfx. aurantiacus* chlorosomes is of the same order as for the LH2 complex of purple bacteria (Herek et al. 2004). This is surprising because an essential amount of proteins forms the LH2 complex. In chlorosomes, proteins are located only in the baseplate and in the protein-lipid sack enveloping the main body. Probably, only those Cars that are located close to the baseplate and the sack mainly contribute to the ultrafast Stark shift, while the other Cars do not. The proximity of these Cars to proteins may be the reason for the rather high value of $|\boldsymbol{E}|$. If it is true, we have a case of photoselection due to the Stark effect. On the other hand, it may simply be a consequence of the limited applicability of formula (4) to the case of ultrafast Stark effect in chlorosomes.

Finally, we tried to estimate the distance R between Car and excited BChl *c*. For the order-of-magnitude estimation, we considered a point dipole with a dipole moment equal to the transition dipole moment of the Q_y band of *Cfx. aurantiacus* chlorosomes. The dipole strength of monomeric BChl c dissolved in methanol is ~ 20 D^2 (Knox and Spring 2003). Comparison of the Q_y dipole strength of chlorosomal and monomeric BChl *c* (e. g. Yakovlev et al. 2020) gives a value of $|\boldsymbol{\mu}| \sim 6\ D$ for chlorosomes. The electric field of a point dipole can be written as (e. g. Benenson et al. 2002):

$$E = \left(\frac{3(\boldsymbol{\mu}\mathbf{r})r}{R^5} - \frac{\mu}{R^3} \right) \tag{5}$$

where $\boldsymbol{r}$ is the distance vector, R is the distance between the dipole and the point of measurement. It can be obtained from formula (5) that the value of dipole electric field is ~ 10^6 V/cm at the distance $R \sim 1$ nm. Obviously, this case is far from reality because neither the excited BChl aggregate nor the Car molecule can be considered as point objects at this distance. Also, the obtained distance of 1 nm seems somewhat large for the known ultrafast ($\tau \leq 100$ fs) EET from Car to BChl *c* in chlorosomes from *Cfx. aurantiacus* (Yakovlev et al. 2021). For example, in RCs of purple bacteria the known Car-to-P distance of 10.5 Å corresponds to $\tau_{EET} = 2.2$ ps (Lin et al. 2003). Assuming the Förster mechanism of this EET, one can calculate that $\tau_{EET} \sim 100$ fs corresponds to the distance of ~ 6 Å. In *Cfx. aurantiacus* chlorosomes, the lack of knowledge on the spectral properties of the very first energy acceptor in Car → BChl *c* EET (some very high-energy exciton or vibrational level of the Q_y or Q_x band) greatly complicates the calculation of the Förster Car-to-BChl *c* distance. In addition, the relative orientation of Car and BChl dipoles in RCs and chlorosomes is obviously not the same which makes difficult a simple comparison of the distances and τ_{EET} between them. Thus, our order-of-magnitude estimation showed that the average Car-to-BChl *c* distance in *Cfx. aurantiacus* chlorosomes is most probably ≤ 1 nm. This estimation can be considered as an upper limit. Obviously, this distance varies noticeably in different structures of BChl aggregates.

The data obtained here permitted us to draw a hypothetical picture of the light-induced Stark shift of the Car absorption band in *Cfx. aurantiacus* chlorosomes. We assumed that Car molecules are uniformly distributed over the chlorosomal body at a distance of ~ 10 Å from the nearest BChl *c* aggregates. It was widely discussed that, most probably, chlorosomal Cars are located between lamellar aggregates (Frigaard and Bryant 2006; Oostergetel et al. 2010; Pšenčik et al. 2004, 2010, 2013) (interlamellar distance ~ 2–4 nm) or inside/between tubular aggregates (Frigaard and Bryant 2006; Oostergetel et al. 2010; Staehelin et al. 1978; Günther et al. 2016; Linnanto and Korppi-Tommola 2008; Sprague et al. 1981) (diameter of rods ~ 10 nm). When excitation arrived to BChl *c*, the majority of Car molecules exhibited a red or a blue shift (depending on their orientation) of the S_0-S_2 absorption band by ~ 15–35 cm^{-1}. Then, complicated processes of exciton migration, delocalization and relaxation occurred in BChl *c* on time-scales from sub-100 fs to sub-ps (Linnanto and Korppi-Tommola 2008, 2012; Dostál et al. 2012; Márquez et al. 2016). During these early-time events, the energy flow is directed toward the baseplate, and the number of Car molecules which feel the electric field of neighboring BChl *c* gradually decreases. These processes are mainly completed during 1–2 ps after excitation, and the main portion of the excitation is concentrated at the bottom of the chlorosome near the baseplate. At this time, only a minor amount of Car molecules, which are located close to the baseplate, exhibited the Stark effect. Later, the slow process of EET to the baseplate BChl *a* occurred on a time scale of ~ 10 ps, but only a small amount of Car feels this. This scenario explains why fast (1–2 ps) components

dominate in the kinetics of the light-induced Stark shift in *Cfx. aurantiacus* chlorosomes.

The spatial organization of BChls in chlorosomes are extensively studied (Frigaard and Bryant 2006; Mirkovic et al. 2017; Oostergetel et al. 2010; Bryant and Canniffe 2018; Krasnovsky and Bystrova 1980; Smith et al. 1983; Staehelin et al. 1978; Pšenčik et al. 2004; Ganapathy et al. 2009; Günther et al. 2016). It is widely accepted that BChls self-organize into 2D lattices which further form different structures such as undulating lamellae, rods, spirals or open half-tubes. There are several arguments in favor of the moderate strength of the light-induced electric field in chlorosomes. The strong exciton coupling between pigments leads to spatial spreading of excitation and, thus, decreases the energy density of the electric field induced by excitation. On the other hand, the absence of a sufficient amount of proteins also prevents the creation of strong local electric fields in chlorosomes. In addition, further reduction of light-induced electric fields can be expected in models of antiparallel stacks of partially overlapping pigments. All of this can result in a rather weak electric field (for example, in comparison with that in the LHCs or RCs of purple bacteria), generated by light excitation, and, as a consequence, a moderate Stark shift of the Car absorption band. Surprisingly, order-of-magnitude estimations based on the general expression (4) showed the same order of magnitude of the light-induced electric field in chlorosomes and LHCs of purple bacteria. This finding needs additional study. It is likely that chlorosomal Cars are not randomly located and oriented, but in an optimal way to ensure their function as photoprotectors and light-harvesters, as, for example, in the LHCs of purple bacteria (see X-ray structure of LHCs from purple bacteria (McDermott et al. 1995; Koepke et al. 1996)). In addition, Stark spectroscopy study of *Cfx. aurantiacus* chlorosomes argues in favor of a moderate participation of Cars in the stabilization of the chlorosomal structure (Frese et al. 1997). The data presented here show a broad variety of orientations of Car molecules with respect to local electric fields generated by light excitation of BChl *c* in chlorosomes from *Cfx. aurantiacus*. We found that about 60% of the Cars exhibited a Stark red shift, and the remaining 40% showed a blue shift of the same magnitude. In chlorosomes, the map of light-induced electric fields likely repeated to some extent the spatial structure of aggregated BChl. The diversity of orientations of Cars with respect to BChl means that Car molecules are not strictly connected to BChl aggregates.

Conclusions

In *Cfx. aurantiacus* chlorosomes, β and γ carotenes are sensitive to internal electric fields induced by light excitation of BChl *c* oligomers. The femtosecond excitation of the Q_y state of BChl *c* creates an electric field in the place of the Car molecules in chlorosome, which leads to an electrochromic shift (Stark effect) of the absorption bands of both carotenes. Using the experimental value of this shift of ~ 15–35 cm^{-1} obtained here, and the Stark spectroscopy data taken from the literature, we estimated the averaged value of the electric field strength as ~ 10^6 V/cm and the averaged distance between Car and the neighboring BChl *c* as ~ 10 Å. The observed value of the electrochromic shift of the Car absorption band in *Cfx. aurantiacus* chlorosomes is several times smaller than in LHCs and RCs containing proteins. We concluded that β and γ carotene contributed equally to the light-induced electrochromic band shift. The dynamics of the Car electrochromic band shift mainly repeated the initial phase of the BChl *c* excited state dynamics, which consists in exciton migration through the chlorosome toward the baseplate. The Car band shift appears simultaneously with the pump pulse and then decays within ~ 1–2 ps. The major (~ 10 ps) component of the BChl *c* Q_y dynamics corresponding to BChl *c* → BChl *a* EET is also reflected by the Car band shift dynamics as a weak minor component. This can be explained by the rather small amount of Car molecules that are sensitive to the electric field created by this component. Our data are compatible with the assumption that the Car molecules are variously oriented with respect to BChl in chlorosomes. Thus, our work has unambiguously shown that Cars are sensitive indicators of light-induced internal electric fields in chlorosomes.

Supplementary Information The online version contains supplementary material available at https://doi.org/10.1007/s11120-022-00942-7.

Acknowledgements We are greatly acknowledged to Prof. Vladimir A. Shuvalov for general support.

Author contributions The authors equally contributed to the present work.

Data availability The data are available from the corresponding author on reasonable request.

Declarations

Conflict of interest The authors have no known competing financial interests or personal relationships that could affect the present work.

References

Benenson W, Harris JW, Stocker H, Lutz H (eds) (2002) Handbook of physics. Springer, New York

Bryant DA, Canniffe DP (2018) How nature designs light-harvesting antenna systems: design principles and functional realization in chlorophototrophic prokaryotes. J Phys B 51:033001

Bublitz GU, Boxer SG (1997) Stark spectroscopy: Applications in chemistry, biology, and materials science. Annu Rev Phys Chem 48:213–242

De Grooth BG, Amesz J (1977) Electrochromic absorbance changes of photosynthetic pigments in Rhodopseudomonas sphaeroides. II. Analysis of the band shifts of carotenoid and bacteriochlorophyll. Biochim Biophys Acta 462:247–258

Dostál J, Mančal T, Augulis R, Vácha F, Pšenčík J, Zigmantas D (2012) Two-dimensional electronic spectroscopy reveals ultrafast energy diffusion in chlorosomes. J Am Chem Soc 34:11611–11617

Frese R, Oberheide U, van Stokkum I, van Grondelle R, Foidl M, Oelze J, van Amerongen H (1997) The organization of bacteriochlorophyll c in chlorosomes from Chloroflexus aurantiacus and the structural role of carotenoids and protein. Photosynth Res 54:115–126

Frese RN, Palacios MA, Azzizi A, van Stokkum IHM, Kruip J, Rögner M, Karapetyan NV, Schlodder E, van Grondelle R, Dekker JP (2002) Electric field effects on red chlorophylls, h-carotenes and P700 in cyanobacterial Photosystem I complexes. Biochim Biophys Acta 1554:180–191

Frigaard N-U, Bryant D (2006) Chlorosomes: antenna organelles in green photosynthetic bacteria. In: Shively JM (ed) Complex intracellular structures in prokaryotes: Microbiology monographs 2. Springer. pp 79–114

Fuciman M, Chábera P, Župčanová A, Hříbek P, Arellano JB, Vácha F, Pšenčík J, Polívka T (2010) Excited state properties of aryl carotenoids. Phys Chem Chem Phys 12:3112–3120

Ganapathy S, Oostergetel G, Wawrzyniak P, Reus M, Gomez Maqueo Chew A, Buda F, Boekema E, Bryant D, Holzwarth A, de Groot H (2009) Alternating syn-anti bacteriochlorophylls form concentric helical nanotubes in chlorosomes. Proc Natl Acad Sci USA 106:8525–8530

Gottfried DS, Steffen MA, Boxer SG (1991a) Large protein-induced dipoles for a symmetric carotenoid in photosynthetic antenna complex. Science 251:662–665

Gottfried DS, Steffen MA, Boxer SG (1991b) Stark effect spectroscopy of carotenoids in photosynthetic antenna and reaction center complexes. Biochim Biophys Acta 1959:76–90

Gradinaru CC, van Grondelle R, van Amerongen H (2003) Selective interaction between xanthophylls and chlorophylls in LHCII probed by femtosecond transient absorption spectroscopy. J Phys Chem B 107:3938–3943

Günther L, Jendrny M, Bloemsma E, Tank M, Oostergetel G, Bryant D, Knoester J, Köhler J (2016) Structure of light-harvesting aggregates in individual chlorosomes. J Phys Chem B 120:5367–5376

Halfen LN, Pierson BK, Francis GW (1972) Carotenoids of a gliding organism containing bacteriochlorophylls. Arch Mikrobiol 82:240–246

Hashimoto H, Uragami C, Yukihira N, Gardiner AT, Cogdell RJ (2018) Understanding/unravelling carotenoid excited singlet states. J R Soc Interface 15:20180026

Herek JL, Polívka T, Pullerits T, Fowler GJS, Hunter CN, Sundström V (1998) Ultrafast carotenoid band shifts probe structure and dynamics in photosynthetic antenna complexes. Biochemistry 37:7057–7061

Herek JL, Wendling M, He Z, Polívka T, Garcia-Asua G, Cogdell RJ, Hunter CN, van Grondelle R, Sundström V, Pullerits T (2004) Ultrafast carotenoid band shifts: experiment and theory. J Phys Chem B 108:10398–10403

Knox RS, Spring BQ (2003) Dipole strengths in the chlorophylls. Photochem Photobiol 77:497–501

Koepke J, Hu X, Muenke C, Schulten K, Michel H (1996) The crystal structure of the light-harvesting complex II (B800–850) from Rhodospirillum molischianum. Structure 4:581–597

Krasnovsky A, Bystrova M (1980) Self-assembly of chlorophyll aggregated structures. BioSystems 12:181–194

Krawczyk S, Olszówka D (2001) Spectral broadening and its effect in Stark spectra of carotenoids. Chem Phys 265:335–347

Lin S, Katilius E, Taguchi AKW, Woodbury NW (2003) Excitation energy transfer from carotenoid to bacteriochlorophyll in the photosynthetic purple bacteria reaction center of Rhodobacter sphaeroides. J Phys Chem B 107:14103–14108

Linnanto JM, Korppi-Tommola JEI (2008) Investigation on chlorosomal antenna geometries: tube, lamella and spiral-type self-aggregates. Photosynth Res 96:227–245

Linnanto JM, Korppi-Tommola JEI (2012) Exciton description of excitation energy transfer in the photosynthetic units of green sulfur bacteria and filamentous anoxygenic phototrophs. J Phys Chem B 117:11144–11161

Liptay W (1974) Dipole moments and polarizabilities of molecules in excited electronic states. In: Lim CE (ed) Excited states, vol 1. Academic Press, New York, pp 129–229

Ma Y-Z, Cox R, Gillbro T, Miller M (1996) Bacteriochlorophyll organization and energy transfer kinetics in chlorosomes from Chloroflexus aurantiacus depend on the light regime during growth. Photosynth Res 47:157–165

Márquez AS, Chen L, Sun K, Zhao Y (2016) Probing ultrafast excitation energy transfer of the chlorosome with exciton–phonon variational dynamics. Phys Chem Chem Phys 18:20298

McDermott G, Prince SM, Freer AA, Hawthornwaite-Lawless AM, Papiz MZ, Cogdell RJ, Isaacs NW (1995) Crystal structure of an integral membrane light-harvesting complex from photosynthetic bacteria. Nature 374:517–521

Meixner AJ, Renn A, Bucher SE (1986) Wild UP (1986) Spectral hole burning in glasses and polymer films: the Stark effect. J Phys Chem 90(26):6777–6785

Melø TB, Frigaard NU, Matsuura K, Naqvi KR (2000) Electronic energy transfer involving carotenoid pigments in chlorosomes of two green bacteria: Chlorobium tepidum and Chloroflexus aurantiacus. Spectrochim Acta A 56:2001–2010

Mirkovic T, Ostroumov EE, Anna JM, van Grondelle R, Govindjee SGD (2017) Light absorption and energy transfer in the antenna complexes of photosynthetic organisms. Chem Rev 117:249–294

Oostergetel GT, van Amerongen H, Boekema EJ (2010) The chlorosome: a prototype for efficient light harvesting in photosynthesis. Photosynth Res 104:245–255

Palacios MA, Frese RN, Gradinaru CC, van Stokkum IHM, Premvardhan LL, Horton P, Ruban AV, van Grondelle R, van Amerongen H (2003) Stark spectroscopy of the light-harvesting complex II in different oligomerisation states. Biochim Biophys Acta 1605:83–95

Paschenko VZ, Gorokhov VV, Korvatovskiy BN, Bocharov EA, Knox PP, Sarkisov OM, Theiss C, Eichler HJ, Renger G, Rubin AB (2012) The rate of $Q_x \rightarrow Q_y$ relaxation in bacteriochlorophylls of reaction centers from Rhodobacter sphaeroides determined by kinetics of the ultrafast carotenoid bandshift. Biochim Biophys Acta 1817:1399–1406

Pinnola A, Staleva-Musto H, Capaldi S, Ballottari M, Bassi R, Polívka T (2016) Electron transfer between carotenoid and chlorophyll contributes to quenching in the LHCSR1 protein from Physcomitrella patens. Biochim Biophys Acta 1857:1870–1878

Polivka T, Sundström V (2004) Ultrafast dynamics of carotenoid excited states—from solution to natural and artificial systems. Chem Rev 104:2021–2072

Prokhorenko VI, Steensgaard DB, Holzwarth AR (2000) Exciton dynamics in the chlorosomal antennae of the green bacteria Chloroflexus aurantiacus and Chlorobium tepidum. Biophys J 79:2105–2120

Pšenčik J, Ikonen T, Laurinmäki P, Merckel M, Butcher S, Serimaa R, Tuma R (2004) Lamellar organization of pigments in chlorosomes, the light harvesting system of green bacteria. Biophys J 87:1165–1172

Pšenčik J, Torkkeli M, Zupčanová A, Vácha F, Serimaa R, Tuma R (2010) The lamellar spacing in self-assembling bacteriochlorophyll aggregates is proportional to the length of the esterifying alcohol. Photosynth Res 104:211–219

Pšenčik J, Arellano J, Collins A, Laurinmäki P, Torkkeli M, Löflund B, Serimaa R, Blankenship R, Tuma R, Butcher S (2013) Structural and functional roles of carotenoids in chlorosomes. J Bacteriol 195:1727–1734

Rätsep M, Wu H-M, Hayes JM, Blankenship RE, Cogdell RJ, Small GJ (1998) Stark hole-burning studies of three photosynthetic complexes. J Phys Chem B 102:4035–4044

Romero E, van Stokkum IHM, Dekker JP, van Grondelle R (2011) Ultrafast carotenoid band shifts correlated with Chlz excited states in the photosystem II reaction center: are the carotenoids involved in energy transfer? Phys Chem Chem Phys 13:5573–5575

Savikhin S, Zhu Y, Lin S, Blankenship RE, Struve WS (1994) Femtosecond spectroscopy of chlorosome antennas from the green photosynthetic bacterium Chloroflexus aurantiacus. J Phys Chem 98:10322–10334

Smith K, Kehres L, Fajer J (1983) Aggregation of bacteriochlorophylls c, d or e. Models for the antenna chlorophylls of green and brown photosynthetic bacteria. J Am Chem Soc 105:1387–1389

Sprague S, Staehelin L, DiBartolomeis M, Fuller R (1981) Isolation and development of chlorosomes in the green bacterium Chloroflexus aurantiacus. J Bacteriol 147:1021–1031

Staehelin L, Golecki J, Fuller R, Drews G (1978) Visualization of the supramolecular architecture of chlorosomes (Chlorobium type vesicles) in freeze-fractured cells of Chloroflexus aurantiacus. Arch Microbiol 119:269–277

Taisova AS, Keppen OI, Lukashev EP, Arutyunyan AM, Fetisova ZG (2002) Study of the chlorosomal antenna of the green mesophilic filamentous bacterium Oscillochloris trichoides. Photosynth Res 74:73–85

Takaichi S (1999) Carotenoids and carotenogenesis in anoxygenic photosynthetic bacteria. In: Frank HA, Young AJ, Britton G, Cogdell RJ (eds) The photochemistry of carotenoids. Kluwer Academic, Dordrecht, The Netherlands, pp 39–69

Yakovlev A, Taisova A, Fetisova Z (2002) Light control over the size of an antenna unit building block as an effecient strategy for light harvesting in photosynthesis. FEBS Lett 512:129–132

Yakovlev AG, Taisova AS, Fetisova ZG (2020) Q-band hyperchromism and B-band hypochromism of bacteriochlorophyll *c* as a tool for investigation of the oligomeric structure of chlorosomes of the green photosynthetic bacterium Chloroflexus aurantiacus. Photosynth Res 146:95–108

Yakovlev AG, Taisova AS, Fetisova ZG (2021) Utilization of blue-green light by chlorosomes from the photosynthetic bacterium Chloroflexus aurantiacus: ultrafast excitation energy conversion and transfer. Biochim Biophys Acta 1862:148396